



## Design and Fabrication of Reduction-Sensitive Cell Penetrating Nanofibers for Enhanced Drug Efficacy

Journal:	<i>Journal of Materials Chemistry B</i>
Manuscript ID	TB-COM-03-2018-000728.R1
Article Type:	Communication
Date Submitted by the Author:	18-Apr-2018
Complete List of Authors:	Yang, Su; University of Texas at Arlington Xu, Dawei; Clarkson University Dong, He; University of Texas at Arlington, Chemistry and Biochemistry



Journal Name

COMMUNICATION

## Design and Fabrication of Reduction-Sensitive Cell Penetrating Nanofibers for Enhanced Drug Efficacy

Received 00th January 20xx,  
Accepted 00th January 20xx

Su Yang,<sup>a</sup> Dawei Xu,<sup>b</sup> and He Dong\*<sup>a, b</sup>

DOI: 10.1039/x0xx00000x

www.rsc.org/

**This work demonstrates a modular design strategy based on the supramolecular assembly of multidomain peptides to fabricate reduction-responsive cell penetrating nanofibers (CPNs), which hold great promise for selective targeting of cancer therapeutics to tumor cells.**

The development of nanomaterials has offered tremendous promise and opportunity for nanocarrier-based cancer therapy which dramatically reduces the toxicity effects of chemotherapeutic drugs on healthy tissues and cells.<sup>1-4</sup> More recently, targeted delivery of cancer therapeutics to diseased sites has attracted great attention to promote the clinical application of functional nanocarriers. Various tumor physiology triggers, such as pH,<sup>5, 6</sup> enzymes,<sup>7, 8</sup> reduction,<sup>9, 10</sup> and hypoxia,<sup>11, 12</sup> have been utilized to activate the nanomaterials at the tumor sites to improve cell uptake and subsequent drug release.

Trigger-responsive nanomaterials can be divided into two classes depending on their sites of activation at the cellular level. One is designed to respond to the physiological triggers in the extracellular matrix where the nanomaterials become highly cell membrane permeable for enhanced cell uptake.<sup>13-15</sup> The second becomes activated only when they are internalized inside cells where nanomaterials are degraded or disassembled to release the therapeutic payloads.<sup>16, 17</sup> Both mechanisms demonstrate great potential in selectively targeting cancer therapeutics to tumor tissues and cells for improved therapeutic effects. Particularly, for trigger-responsive membrane active nanoparticles, efforts have been made to modify the surface chemistry of the drug delivery systems by incorporating membrane pro-active components, such as protected cell penetrating peptides (CPPs).<sup>18-20</sup> The membrane activity of CPP functionalized system is greatly enhanced upon CPP activation in the presence of tumor-specific triggers leading to improved cell uptake and drug efficacy. However, the fabrication of such systems often involves the use of multi-component building blocks and may require stringent quality control for both the

synthesis and formulation process. Therefore, it is desirable to develop new design principles and chemical methods to generate trigger-responsive materials that are structurally simple, easy to fabricate and modulate, and highly membrane penetrable for effective cancer treatment.

We have previously reported a membrane-active peptide nanofiber based on the self-assembly of multidomain peptides (MDPs) with a general sequence of  $K_x(QW)_y$ , where  $x$  represents the numbers of lysine (K) residues and  $y$  represents the numbers of alternating glutamine (Q) and tryptophan (W) repeating units.<sup>21, 22</sup> The alternating polar and nonpolar residue pattern provides the driving force for  $\beta$ -sheet formation and their packing into supramolecular nanofibers while the lysine residues are displayed at the fiber surface to interact with the cell membrane. We previously studied the self-assembly process of MDPs and showed the significance of the interplay between peptide self-assembly and cell penetrating activity. Nanofibers composed of  $K_{10}(QW)_6$  showed a good balance between supramolecular packing and charge domain flexibility which is a critical factor for achieving optimal cell uptake and transport of membrane-impermeable molecules. In this work, we will utilize the unique membrane activity of these self-assembled nanofibers and fabricate a trigger-responsive cell penetrating nanofiber (TR-CPN) using integrated MDPs where each individual component is amenable to change to tune the nanostructure and biological activity for targeted cancer therapy.

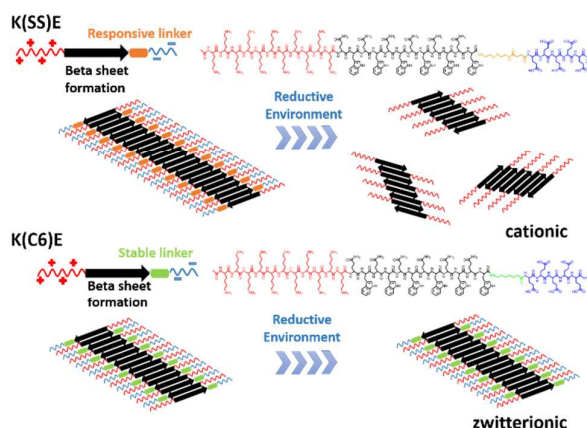
For proof-of-concept, we focus on the design and fabrication of TR-CPNs that are sensitive to reductive chemical environment, which has been used to differentiate tumor tissues and cells from normal ones.<sup>23-25</sup> **Scheme 1** shows the chemical structure of the reduction-sensitive MDP with a sequence of  $K_{10}(QW)_6(SS)E_5$ , abbreviated as  $K(SS)E$  where  $SS$  refers to the reduction sensitive linker which was synthesized according to the procedure published by Yang *et al.*<sup>26</sup> and can be readily programmed in the solid phase peptide synthesis. Five glutamic acids were included at the C-terminus to have self-complementary ionic interactions with the lysine residues. Upon self-assembly,  $E_5$  and  $K_{10}$  domain are aligned along the fiber axis as dictated by the intrinsic packing order of the MDPs within the supramolecular assembly (**Scheme 1**). The polyanionic ( $E_5$ ) and polycationic ( $K_{10}$ ) are stacked over one another so that the positive charges are partially screened, therefore the membrane activity of the nanofiber is reduced. Upon removal of the  $E_5$  domain under the reductive condition, the effective positive charges at the fiber surface will increase and the

<sup>a</sup> Department of Chemistry and Biochemistry, The University of Texas at Arlington, Arlington, TX, 76019, USA. Email: he.dong@uta.edu

<sup>b</sup> Department of Chemistry and Biomolecular Science, Clarkson University, Potsdam, NY, 13699, USA.

† Electronic Supplementary Information (ESI) available: peptide synthesis and HPLC purification, confocal microscopy and CCK8 assay for cytotoxicity. See DOI: 10.1039/x0xx00000x

membrane activity of the assembly can be retrieved. Jiang *et al.* demonstrated the design of fusion activatable CPPs where enzymatic cleavage of a  $\beta$ -hairpin linker between the polycationic and polyanionic domain released the CPP portion and its attached cargo to bind to and enter cells.<sup>14</sup> The supramolecular assembly of  $\beta$ -sheet peptides provides an alternative strategy to control the position and interaction of the polyanionic domain, E5 with the polycationic lysine domain upon self-assembly and further mediate their membrane activity. Collier's group recently studied the effect of surface charges on the supramolecular peptide nanofibers on eliciting antibody production and T cell responses.<sup>27</sup> It was found that positively charged surface can augment uptake of materials by antigen presenting cells while negatively charged surface prevented uptake. Cui and Azevedo recently demonstrated enzymatic activation of cell penetrating peptides as the nanofibers transitioned to spherical micelles.<sup>13</sup> We will take advantage of the existing discovery and incorporate both positive and negative surface design parameters into a single nanofiber formulation to fabricate smart, tumor-responsive cell penetrating nanomaterials. Based on our results, five glutamic acids are sufficient to shield the lysine residues and show selectivity under the reductive condition. However, the numbers of glutamic acids can be readily changed to tune the nanostructure and membrane activity as needed. A control MDP (**Scheme 1**) was synthesized by replacing the SS moiety with a non-responsive linker and the sequence is referred as  $K_{10}(QW)_6(C6)E_5$ , abbreviated as K(C6)E. Although current peptides are designed to be reduction-sensitive, the design principle can be readily applied to the synthesis and formulation of other types of TR-CPNs, such as enzymatic responsive CPNs by integrating oligopeptide substrates for various tumor-specific enzymes in the MDPs for targeted cancer therapeutics delivery.



**Scheme 1** Color-coded chemical structure and cartoon representation of reduction-sensitive and non-sensitive MDPs and their self-assembly into supramolecular nanofibers. Red: K10 as the polycationic domain; Black: (QW)<sub>6</sub> to drive the supramolecular packing of  $\beta$ -sheet nanofiber; Blue: E5 as the polyanionic domain; Orange: reduction-sensitive linker; Green: non-sensitive linker.

K(SS)E and K(C6)E were designed to undergo spontaneous self-assembly into  $\beta$ -sheet nanofibers in Tris buffer (pH=7.4, 20 mM). To monitor the solution assembly behavior, we first determined the critical assembly concentrations (CACs) of both peptides using a previously established method where fluorescence intensity of the peptides was measured as a function of peptide concentration.<sup>28, 29</sup> Due to the packing of  $\beta$ -sheets, tryptophan residues are in spatial

proximity relative to one another in the hydrophobic core such that the change of the fluorescence intensity falls off the linear range and the cross point between the two regions is defined as the CAC (**Fig. S1**). The CACs for K(SS)E and K(C6)E are 9.1  $\mu$ M and 7.9  $\mu$ M respectively. For all structural characterization and biological activity measurements, peptide concentrations were above their CACs to form supramolecular nanofibers. To study the response of peptides toward the reductive environment, the assembled peptides in aqueous buffer were treated with a reducing agent dithiodithreitol (DTT) and the reduction product was analyzed by mass spectrometry. The DTT concentration used in the solution study was based on clinical studies of glutathione levels in human tumors that showed a typical range from 0.5 to 3 mM in for example brain tumors along with several other cancers.<sup>30</sup> Based on the MALDI results (**Fig. S2**), K(SS)E was completely degraded upon the addition of DTT leading to a reduced molecular weight of a peptide fragment at 3291 while the original peptide wasn't detected. The near complete degradation of K(SS)E was confirmed by analytical HPLC where a peak shift of DTT-treated peptide was clearly observed compared to the peptide before DTT addition (**Fig. S2**). The control peptide, K(C6)E, remained intact upon DTT treatment (**Fig. S3**).

Next, the molecular structures of the peptides were studied by circular dichroism (CD) spectroscopy under the reductive condition in the presence DTT. **Fig. 1a** showed the CD spectra of K(SS)E before and after DTT treatment for 1 hr at 37 °C. Before adding DTT, K(SS)E adopted a predominant  $\beta$ -sheet structure as characterized by the minimum peak at 213 nm. Upon the addition of DTT, a new peak at 208 nm appeared suggesting part of the  $\beta$ -sheets transitioned to  $\alpha$ -helices. As mentioned above, E5 is used to stabilize the  $\beta$ -sheet packing by electrostatic interactions with K10. The increased helical content is presumably due to the removal of the E5 domain so that K10 becomes more flexible to form  $\alpha$ -helices (It is known that polylysine can form all three commonly occurring protein secondary structures depending on the environmental condition). There is possibility that E5 may still be attached at the fiber surface upon cleavage. Therefore, we performed zeta potential measurements to confirm the surface charges upon DTT treatment. To minimize potential structural reorganization of the nanofibers upon exposure to the electric field, we took the average of the zeta potential readings from the first three measurements of each sample for fair comparison. As shown in **Fig. 1b**, the zeta potential of self-assembled peptides increased from 17.5 mV to 25 mV upon the addition of DTT, suggesting the recovery of the positive charges on the nanofiber surface after disulfide bond was cleaved. The cleaved product has a zeta potential value close to the positive control peptide, referred as  $K_{10}(QW)_6$  at 28 mV. Based on the cell-based assay results as will be discussed later, any residual E5 did not seem to pose a significant barrier for the peptide nanofiber to interact with the cell membrane for drug transport. The cell penetrating activity and therapeutic delivery efficacy was dramatically enhanced for the responsive peptide compared with the non-responsive peptide in HeLa cell culture.

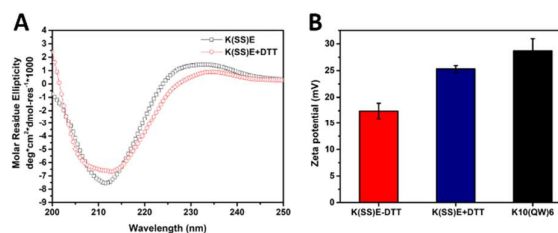


**Fig. 1 (A)** CD spectra of K(SS)E in the presence and absence of DTT. **(B)** Zeta potential of K(SS)E upon DTT treatment. Peptide concentration: 100  $\mu$ M in Tris buffer (20 mM, pH =7.4). DTT concentration: 1 mM in Tris buffer (20 mM, pH =7.4).

In comparison to K(SS)E, the CD spectra of the non-responsive peptide, K(C6)E was essentially unchanged upon DTT addition (**Fig. S4**). It is also worth noting that CD spectroscopy only provides the information about the global secondary structures, and is limited in its ability to decouple the local secondary structure of each segment/amino acid. The detailed molecular conformation of amino acids in each domain can be determined through both solution and solid-state NMR spectroscopy which will be our primary focus in future.

The self-assembled nanostructure of the responsive peptide was examined by negatively stained transmission electron microscopy (TEM). Without DTT, peptides form nanofibers of relatively defined morphology with minimum twisting and deformation (**Fig. 2a**). A statistical measurement based on a total of one hundred randomly selected nanofibers yielded an average length of 80 nm and uniform diameter at 5 nm for self-assembled K(SS)E (**Fig. 2b**). The addition of DTT dramatically reduced the fiber length to 50 nm (**Fig. 2d**) and a large fraction of defects were observed on the nanofibers after reduction (**Fig. 2c**). The change of nanostructure can be correlated to the change of molecular secondary structures shown on the CD spectra. Upon removal of the E5 domain, the cationic domain of K10 repels each other and the repulsive force will compromise the molecular packing of  $\beta$ -sheet nanofibers, leading to local defects and overall fiber length reduction. The structure of self-assembled K(C6)E was also characterized in the presence and absence of DTT. As shown in **Fig. S5**, K(C6)E self-assembled into nanofibers and the size and morphology did not change much upon the addition of DTT. Based on the statistical size analysis, the length of the K(C6)E nanofibers were much shorter than those of K(SS)E before reduction, yet comparable to those of reduced ones. We speculate the morphological difference between K(C6)E and K(SS)E before reduction is due to the chemical nature of the linker used to connect the cationic and anionic domain. The SS linker has two additional amide groups that may strengthen the intermolecular hydrogen bonding network along the fiber axis. Instead, the hexyl group in the C6 linker is more flexible and such local flexibility is likely to cause steric hindrance for the intermolecular packing of peptide subunits along the fiber axis. Although K(C6)E formed nanofibers of smaller sizes, it is not membrane-active presumably because of the charge screening effect. In our previous publication,<sup>21</sup> we explored the cell penetrating activity of nanofibers of different lengths but comparable cationic charge density. We found that given comparable surface charges, small nanofibers showed improved membrane activity. Combining the results of both studies, we believe that the enhanced membrane activity of the reduced K(SS)E nanofibers is due to a combined effect of charge and morphology.

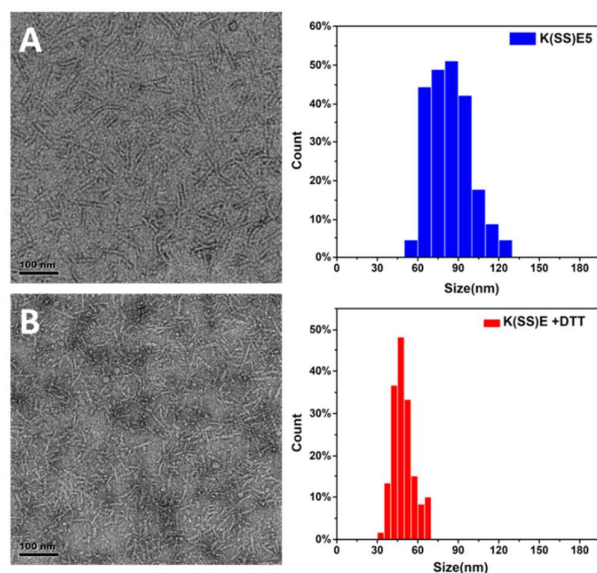


**Fig. 2** TEM images of the nanofibers formed by K(SS)E incubated without **(A)** and with **(B)** DTT. Statistical measurements of length and length distribution of K(SS)E nanofibers without **(C)** and with **(D)** DTT based on a total number of 100 fibers. Scale bar: 100 nm.

The membrane activity of K(SS)E under the reductive condition was investigated *in vitro* by using HeLa cells as a model cancer cell line. Cancer cells are known to produce much higher concentrations glutathione (GT) in both cytoplasm and extracellular matrix which can be used as a tumor-specific trigger to achieve selective delivery of cancer therapeutics.<sup>31,32</sup> For all the *in vitro* cell-based assay, no exogenous reducing agents were added because of the presence of free thiol groups ranging from 0.5 to 1.0 mM in the culture media produced by the HeLa cells as determined by the Elman's test. In this experiment, we investigated and compared the cell uptake of K(SS)E and K(C6)E by monitoring the intracellular fluorescence of fluorescein (FITC)-labeled peptides at 2 hrs and 24 hrs time points through confocal laser scanning microscopy (CLSM) and flow cytometry. A marked difference of cell uptake was observed upon 2 hrs of incubation of peptides with HeLa cells. K(SS)E was internalized to a much larger extent than that of K(C6)E as demonstrated by both CLSM and flow cytometry results (**Fig. 3a** and **3b**). Extended incubation promoted higher uptake of the control peptide (**Fig. S6**), but the reduction-sensitive peptide still showed higher fluorescence intensity than that of the non-responsive peptide. In our work, the peptide is designed to respond to the extracellular GT of tumor tissues and becomes membrane-active in the extracellular matrix upon removal of the capping domain of E5. However, we cannot exclude the possibility of other routes where peptide nanofibers may first attach on the cell membrane and is cleaved by the intracellular GT to be activated for increased cell uptake. Regardless the sites of cleavage and activation, because tumor tissues are known to express much higher amounts of GT than normal tissues, nanofibers composed of reduction-sensitive K(SS)E are highly promising nanocarriers for targeted cancer therapy.



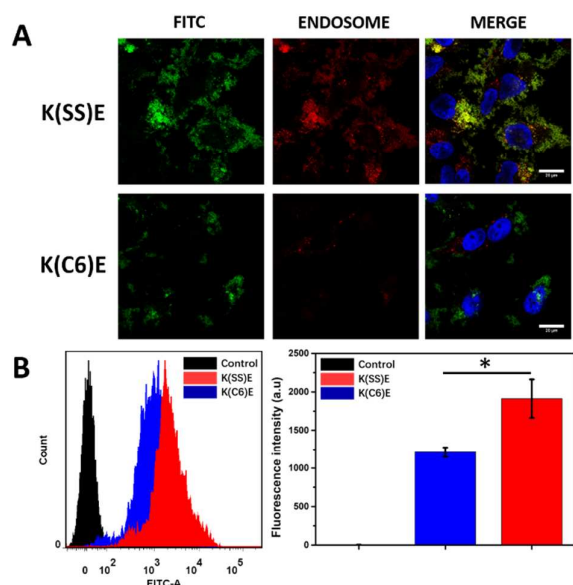


**Fig. 3** (A) Confocal images of the cell uptake of FITC-labeled K(SS)E and K(C6)E upon incubation with HeLa cells for 2 hrs. (B) Cell uptake of K(SS)E and K(C6)E as measured by flow cytometry. Scale bar: 20  $\mu\text{m}$ . Peptide concentration: 16  $\mu\text{M}$ . Statistically significant differences are indicated by  $*p \leq 0.05$ .

To further validate the reduction-sensitive nanofiber platform for targeted therapeutics delivery, we conducted an in vitro cell toxicity assay where a model anticancer drug, membrane impermeable Doxorubicin (DOX, in the form of HCl salt) was co-incubated with three different nanofibers in HeLa cell culture. As shown in our previous work, minimum physical or chemical interaction occurred between DOX and peptides. The purpose of the experiment is to test the ability of various peptide nanofiber systems to perturb the cell membrane, thus allowing the uptake of membrane-impermeable drug molecules to kill cancer cells. We hypothesize that DOX toxicity toward HeLa cells is dictated by the membrane activity of different nanofibers that can potentially perturb the cell membrane to facilitate the transport of DOX to kill cancer cells. Three peptides used in the study include (1) K(SS)E as a reduction-sensitive formulation, (2) K(C6)E as a non-responsive and membrane-inactive formulation, and (3) K<sub>10</sub>(QW)<sub>6</sub> (abbreviated as K10) as a non-selective but membrane-active formulation. The peptide concentration in cell culture media was fixed at 16  $\mu\text{M}$  which is above their CACs and DOX concentrations span from 0.05  $\mu\text{M}$  to 4  $\mu\text{M}$ . Cell viability was evaluated using CCK-8 assay and the IC(50) values of DOX were calculated for each formulation through sigmoidal fitting of the cell viability results (Fig. 4). The IC(50) value of DOX alone is determined at 2.7  $\mu\text{M}$  (Fig. S7), which was reduced to 0.48  $\mu\text{M}$  upon the addition of K(SS)E, suggesting improved drug efficacy. To note, the IC(50) value of K(SS)E is slightly higher than that of K10 (at 0.3  $\mu\text{M}$ ). This is presumably caused by the residual glutamic acids that could be weakly attached on the nanofiber after cleavage to partially shield the membrane interaction of the nanofibers, therefore slightly diminishing the cell penetrating activity. K(C6)E, as a non-responsive formulation and negative control, mimicked the behavior of peptides in normal tissues where the peptides are not subject to cleavage. Although the control formulation still underwent cell uptake as shown by the confocal microscopy and flow cytometry (Fig. 3A and 3B), the interference of

peptide nanofibers to the cell membrane was minimum to cause significant toxicity enhancement.

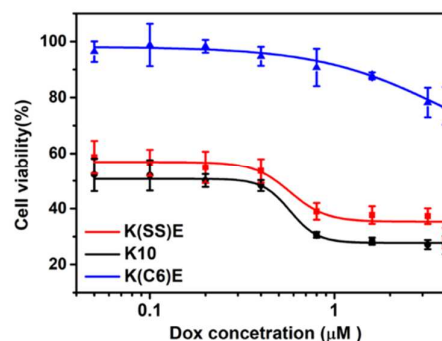


**Fig. 4** HeLa cell viability upon 24 hrs of incubation with DOX in the presence of K(SS)E, K(C6)E and K10. All three peptide concentrations are fixed at 16  $\mu\text{M}$  and DOX concentrations span from 0.05 to 4  $\mu\text{M}$ .

An intriguing phenomena was observed, that is the IC(50) value of DOX in the presence K(C6)E appeared to be higher than that of DOX alone. The result suggested that the uptake of DOX was inhibited upon the addition of the intact supramolecular nanofibers which is expected to exist in the healthy tissues and cells. The mechanistic origin of this unusual effect is largely unknown, but certainly deserve additional research efforts to understand. Further validation of the results using other small molecule drugs will help justify the current design system in terms of its capability to protect the health tissues and cells from passive uptake of cancer therapeutics. Secondly, the cell viability of K(SS)E and K10 alone was estimated at 70% and 81% while K(C6)E showed 97% after 24 hrs of incubation with HeLa cells (Fig. S8). The moderate cytotoxicity is generally recognized when designing cationic peptides/lipids/polymers.<sup>33, 34</sup> However, in this work, the cytotoxicity of the reduction-responsive cell penetrating nanofiber may not be a significant concern as it is expected to function only in tumor tissues where the cell penetrating activity is triggered. In healthy tissues, it is mostly dormant and is not expected to be cytotoxic as shown in the case of non-responsive formulation based on K(C6)E.

## Conclusions

In conclusion, we designed a new class of supramolecular materials based on the self-assembly of  $\beta$ -sheet forming MDPs with tunable nanostructure and cell penetrating activity in response to reduction triggers. Due to the supramolecular packing order of the MDPs, the anionic and cationic were juxtaposed at the periphery of the nanofiber where the lysine residues are partially neutralized within the assembly. Trigger-responsive removal of the polyanionic allows deshielding of the positive charges on the nanofiber and led to reduction of the fiber length. The newly produced short nanofibers demonstrated superior cell penetrating activity for improved drug efficacy upon co-incubation of membrane-impermeable drug molecules with the reduction-sensitive nanofibers in HeLa cell culture. Although current peptides are designed to be reduction-sensitive, the cleavable linker is amenable to change to generate nanofibers in response to other types of responsive triggers in diseased tissues and cells. The modular

nature of the MDPs and the solid phase synthesis method allows easy incorporation of non-natural amino acids or synthetic polymers into the system to overcome the structural limitation associated with natural amino acids. This study is expected to provide important guidelines for the design of peptide-based trigger-responsive nanofibers to suit various needs in biomedical applications.

### Conflicts of interest

There are no conflicts to declare.

### Acknowledgements

This work was supported by National Science Foundation (DMR 1654426).

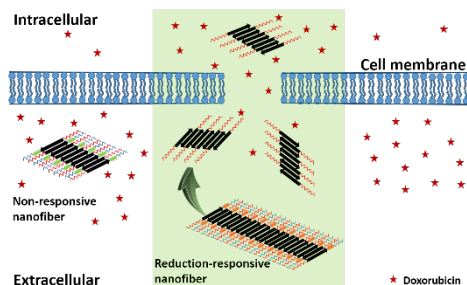
### Notes and references

1. V. P. Torchilin, *Adv. Drug Deliv. Rev.*, 2012, **64**, 302-315.
2. R. A. Petros and J. M. DeSimone, *Nat. Rev. Drug Discov.*, 2010, **9**, 615-627.
3. D. Peer, J. M. Karp, S. Hong, O. C. Farokhzad, R. Margalit and R. Langer, *Nat. Nanotechnol.*, 2007, **2**, 751-760.
4. O. C. Farokhzad and R. Langer, *Adv. Drug Deliv. Rev.*, 2006, **58**, 1456-1459.
5. S.-J. Tseng, Z.-X. Liao, S.-H. Kao, Y.-F. Zeng, K.-Y. Huang, H.-J. Li, C.-L. Yang, Y.-F. Deng, C.-F. Huang, S.-C. Yang, P.-C. Yang and I. M. Kempson, *Nat. Commun.*, 2015, **6**, 6456.
6. Z. Poon, D. Chang, X. Zhao and P. T. Hammond, *ACS Nano*, 2011, **5**, 4284-4292.
7. L. Zhu, T. Wang, F. Perche, A. Taigind and V. P. Torchilin, *Proc. Natl. Acad. Sci. U. S. A.*, 2013, **110**, 17047-17052.
8. S. Huang, K. Shao, Y. Liu, Y. Kuang, J. Li, S. An, Y. Guo, H. Ma and C. Jiang, *ACS Nano*, 2013, **7**, 2860-2871.
9. Z. Luo, X. Ding, Y. Hu, S. Wu, Y. Xiang, Y. Zeng, B. Zhang, H. Yan, H. Zhang and L. Zhu, *ACS Nano*, 2013, **7**, 10271-10284.
10. S. S. Dunn, S. Tian, S. Blake, J. Wang, A. L. Galloway, A. Murphy, P. D. Pohlhaus, J. P. Rolland, M. E. Napier and J. M. DeSimone, *J. Am. Chem. Soc.*, 2012, **134**, 7423-7430.
11. T. Thambi, V. Deepagan, H. Y. Yoon, H. S. Han, S.-H. Kim, S. Son, D.-G. Jo, C.-H. Ahn, Y. D. Suh and K. Kim, *Biomaterials*, 2014, **35**, 1735-1743.
12. F. Perche, S. Biswas, T. Wang, L. Zhu and V. Torchilin, *Angew. Chem., Int. Ed.*, 2014, **126**, 3430-3434.
13. Y. Shi, Y. Hu, G. Ochbaum, R. Lin, R. Bitton, H. Cui and H. S. Azevedo, *Chem. Commun.*, 2017, **53**, 7037-7040.
14. T. Jiang, E. S. Olson, Q. T. Nguyen, M. Roy, P. A. Jennings and R. Y. Tsien, *Proc. Natl. Acad. Sci. U. S. A.*, 2004, **101**, 17867-17872.
15. T. Jiang, Z. Zhang, Y. Zhang, H. Lv, J. Zhou, C. Li, L. Hou and Q. Zhang, *Biomaterials*, 2012, **33**, 9246-9258.
16. L. Rajendran, H.-J. Knölker and K. Simons, *Nat. Rev. Drug Discov.*, 2010, **9**, 29-42.
17. H. Wei, R.-X. Zhuo and X.-Z. Zhang, *Prog. Polym. Sci.*, 2013, **38**, 503-535.
18. K. Fosgerau and T. Hoffmann, *Drug Discov. Today*, 2015, **20**, 122-128.
19. S. Deshayes, M. Morris, G. Divita and F. Heitz, *Cell Mol. Life Sci.*, 2005, **62**, 1839-1849.
20. B. Gupta, T. S. Levchenko and V. P. Torchilin, *Adv. Drug Deliv. Rev.*, 2005, **57**, 637-651.
21. D. Xu, D. S. Samways and H. Dong, *Bioactive Mater.*, 2017, **2**, 260-268.
22. D. Xu, D. Dustin, L. Jiang, D. S. Samways and H. Dong, *Chem. Commun.*, 2015, **51**, 11757-11760.
23. E. Fleige, M. A. Quadir and R. Haag, *Adv. Drug Deliv. Rev.*, 2012, **64**, 866-884.
24. W. Chen, P. Zhong, F. Meng, R. Cheng, C. Deng, J. Feijen and Z. Zhong, *J. Control. Release*, 2013, **169**, 171-179.
25. D. Steinhilber, A. L. Sisson, D. Mangoldt, P. Welker, K. Licha and R. Haag, *Adv. Funct. Mater.*, 2010, **20**, 4133-4138.
26. C. Ren, Z. Song, W. Zheng, X. Chen, L. Wang, D. Kong and Z. Yang, *Chem. Commun.*, 2011, **47**, 1619-1621.
27. Y. Wen, A. Waltman, H. Han and J. H. Collier, *ACS Nano*, 2016, **10**, 9274-9286.
28. D. Xu, Q. Ran, Y. Xiang, L. Jiang, B. M. Smith, F. Bou-Abdallah, R. Lund, Z. Li and H. Dong, *RSC Adv.*, 2016, **6**, 15911-15919.
29. Y. Chen and M. D. Barkley, *Biochemistry*, 1998, **37**, 9976-9982.
30. M. P. Gamcsik, M. S. Kasibhatla, S. D. Teeter and O. M. Colvin, *Biomarkers*, 2012, **17**, 671-691.
31. M. Yang, D. Xu, L. Jiang, L. Zhang, D. Dustin, R. Lund, L. Liu and H. Dong, *Chem. Commun.*, 2014, **50**, 4827-4830.
32. D. Xu, L. Jiang, A. Singh, D. Dustin, M. Yang, L. Liu, R. Lund, T. J. Sellati and H. Dong, *Chem. Commun.*, 2015, **51**, 1289-1292.
33. H. Lv, S. Zhang, B. Wang, S. Cui and J. Yan, *J. Control. Release*, 2006, **114**, 100-109.
34. M. Breunig, U. Lungwitz, R. Liebl and A. Goepferich, *Proc. Natl. Acad. Sci. U. S. A.*, 2007, **104**, 14454-14459.

## Graphical Abstract

Design and Fabrication of Reduction-Sensitive Cell Penetrating Nanofibers For  
Enhanced Drug Efficacy

Su Yang, Dawei Xu, He Dong\*



In this work, we report the facile preparation of reduction-responsive cell penetrating nanofibers through the design and self-assembly of integrated multidomain peptides that have tunable surface charges and nanostructures in response to a chemically reducing environment. Stimuli-responsive cell penetrating activity was demonstrated for improved drug efficacy in HeLa cell culture compared to the non-responsive nanofibers.